Contrasting Rhizospheric and Heterotrophic Components of Soil Respiration during Growing and Non-Growing Seasons in a Temperate Deciduous Forest

Zhen Jiao and Xingchang Wang *

Center for Ecological Research, Northeast Forestry University, Harbin 150040, China; ecozhen0811@163.com
* Correspondence: xcwang_cer@nefu.edu.cn; Tel.: +86-451-8219-0615

Abstract: The contributions of heterotrophic respiration (R_H) to total soil respiration (R_S) for the non-growing season, growing season, and annual period are 84.8%, 60.7%, and 63.3%, respectively. Few studies have partitioned R_S into its rhizospheric (R_R) and heterotrophic components throughout the year in northern forest ecosystems. Our objectives were to quantify the contributions of non-growing season and heterotrophic respiration. We conducted a trenching experiment to quantify R_R and R_H in a temperate deciduous forest in Northeast China over two years using chamber methods. Temperature sensitivities (Q_{10}) for R_S and for R_H were both much higher in the non-growing season (November to April) than those in the growing season. The Q_{10} for R_S was higher than Q_{10} for R_H in both seasons, indicating a higher temperature sensitivity of roots versus microorganisms. Mean non-growing season R_S, R_H, and R_R for the two years were 94, 79 and 14 g carbon (C) m^{-2}, respectively, which contributed 10.8%, 14.5%, and 4.5% to the corresponding annual fluxes (869, 547 and 321 g C m^{-2} year^{-1}, respectively). The contributions of R_H to R_S for the non-growing season, growing season, and annual period were 84.8%, 60.7%, and 63.3%, respectively. Using the same contribution of non-growing season R_S to annual R_S, to scale growing season measurements, to the annual scale would introduce significant biases on annual R_H (-34 g C m^{-2} yr^{-1} or -6%) and R_R (16 g C m^{-2} yr^{-1} or 5%). We concluded that it was important to take non-growing season measurements in terms of accurately partitioning R_S components in northern forests.

Keywords: heterotrophic respiration; autotrophic respiration; temperature sensitivity; non-growing season; temperate forest

1. Introduction

Soil respiration (R_S) is estimated to be 83–108 Pg carbon (C) yr^{-1} globally [1–3], which consumes 67%–88% of the terrestrial gross primary production (123 Pg C yr^{-1}) [4]. In addition, R_S is potentially an important positive feedback for climate warming [5–7]. Thus, R_S plays an essential role in global carbon cycling.

Soil respiration is overwhelmingly comprised of heterotrophic (R_H; respiration by microbes and soil fauna) and rhizospheric (R_R; respiration by roots, their associated mycorrhizal fungi, and other micro-organisms directly dependent on labile carbon compounds leaked from roots) components [8–10]. R_R and R_H may be driven by different mechanisms [8,11], and thus respond differently to environmental factors, both at given sites [8,12,13] and globally [14,15]. Partitioning R_S is an important step for assessing plant physiology, C allocation, ecosystem C balance, and the climate feedback potential of changes in R_S [5,15–17].

Most R_S measurements in northern forests are limited in the growing season [18]. The lack of R_S studies during the non-growing season is due not only to the misconception that there is little biological activity during this period, but also to the inherent difficulties associated with cold winter sampling over snowpack [19]. However, soil respiration has been shown to continue throughout the winter in a wide variety of northern or alpine ecosystems [18,20–24]. Studies which have integrated R_H contribution to R_S throughout an entire year or growing season show a mean value of 54% for the forest ecosystem [9].The relative contributions of R_R and R_H vary during the year [25–32]. In cold climates, the R_H contribution is commonly lower than or similar to that of R_R during the growing season, and higher during the dormant periods. However, few measurements quantified R_H contribution during the winter, particularly for the snow-covered period in northern or alpine ecosystems [25,27,33,34].

There are several methods for partitioning R_S, each with advantages and limitations [9,16,35,36]. The trenching experiment is the most popular method used in boreal and temperate forest ecosystems [35], because of its simplicity and low cost [9]. Soil respiration has been partitioned by the trenching method for six forest ecosystems in the Maoershan site during growing season [28], but no direct measurements were conducted during the non-growing season [24]. In this study, the trenching approach was used throughout two successive years in a broadleaved deciduous forest. We hypothesized that using a same value of root contribution as growing season measurements throughout annual cycles would introduce significant biases in the estimating of annual R_S and its components.

2. Materials and Methods

2.1. Experimental Design and Field Measurements

This study was conducted at the Maoershan Forest Ecosystem Research Station of Northeast Forestry University, Heilongjiang Province, Northeast China (45°24′ N, 127°40′ E, 400 m a.s.l.). The climate is a continental monsoon climate with a windy and dry spring, a warm and humid summer, and a dry and cold winter. The mean (1989–2009) annual precipitation is 629 mm, and mean annual air temperature is 3.1 °C. The mean January and July air temperatures are −18.5 °C and 22.0 °C, respectively [24]. The broadleaved deciduous forest around the eddy flux tower was ~60-years old. The dominant tree species include *Ulmus japonica* Sarg., *Fraxinus mandshurica* Rupr., *Betula platyphylla* Suk., *Populusdavidiana* Dode, *Juglans mandshurica* Maxim., etc. [37]. The soil is a type of alfisol with a parent rock of granite.

Eight 20 m × 30 m plots were set up around the eddy flux tower in August 2007. We measured R_S during the growing season for all plots, and three plots (plot number 2–4) for the non-growing season. The basic stand characteristics were given in Table 1.

Table 1. Basic stand characteristics, soil organic carbon, and total nitrogen for the three plots.

Plot Number	BA m² m⁻²	Biomass Mg ha⁻¹	Litterfall g m⁻² yr⁻¹	FRB g m⁻²	FRN g m⁻²	SOC mg g⁻¹	TN mg g⁻¹	SOC Density Mg ha⁻¹	TN Density Mg ha⁻¹
2	19.54	155.09	459.52	330.33	253.73	97.51	9.81	92.22	9.28
3	26.08	147.04	469.02	237.82	267.28	56.86	7.51	68.91	9.10
4	20.74	142.36	447.49	304.34	298.27	50.68	6.63	66.95	8.76

Basal area (BA) and biomass data were from 2010. Litterfall was the mean of five 1-m² traps per plot [38,39] in 2010 and 2011. Fine root (diameter ≤ 2 mm) biomass (FRB) and fine root necromass (FRN) of the top 40 cm of soil were estimated by eight 10-cm diameter root cores per plot in the summer of 2008. Soil organic carbon (SOC) and total nitrogen (TN) of the top 20 cm were measured in 2016 [40].

Four 100-cm diameter trenched subplots were established in each plot by digging a trench (30 cm wide) around the outside boundary to a depth of 80 cm in October 2007. Trenches were lined with plastic sheets to prevent root entry and potential lateral CO_2 transport [41], and refilled and packed carefully with the same soil. Eight polyvinyl chloride (PVC) collars (10.2 cm inside diameter, 6 cm height) were randomly placed for R_S measurements in each plot, and one collar was installed in each trenched subplot for R_H measurements.

Since May of 2008, soil surface CO_2 effluxes for control plots (R_S) and trenching subplots (R_H) were measured using an LI-COR 6400 portable infrared gas analyzer (IRGA) (LI-COR 6400, LI-COR Inc., Lincoln, NE, USA) equipped with a dynamic chamber (LI-COR 6400-9, LI-COR Inc., Lincoln, NE, USA) bi-weekly to monthly during the growing season. The measurement protocol (three cycles based on a change of 5 µmol mol^{-1} CO_2, subsequently averaged at each collar) was similar to that used in previous soil respiration studies at this site [28,42]. Soil temperatures at 5 cm depth (T_5) and 10 cm depth (T_{10}) was simultaneously measured by a digital thermocouple, and the soil volumetric water content at the top 10 cm depth was detected by a Time-Domain Reflectometry (CS620, Campbell Scientific, Logan, UT, USA).

During the non-growing season, other chamber methods were adopted to measure the R_S and R_T because of LI-COR 6400 failure at low temperatures. A dark static chamber method was used from December 2009 to April 2010. Four steel collars (40 cm wide × 50 cm length) were installed in October 2009 in each plot, and the other four collars were installed in the four trenched subplots. A small vent in the chamber was used to balance the air pressure inside and outside the chamber [43]. Before each measurement, the snow around the base was removed carefully to minimize disturbance of the snow over the base. The stainless-steel statistic chamber (40 cm wide ×50 cm length × 50 cm height) was fitted to the collarand sealed with adhesive tape. Then the snow was quickly refilled to minimize the potential CO_2 pulse from the snow hollow around the chamber base and insulate the soil from the cold air. The chamber was covered by a specific white quilt to prevent heating by solar radiation. A small fan was used to mix the gas in the chamber. Fifty mL gas samples were collected using fine needle syringes 0, 10, 20, and 30 min following placement of the chamber on the base [44]. Snow depth (D_S), T_5, and T_{10} near each chamber were also measured with a ruler and a thermocouple, respectively. Samples were transferred to evacuated gaseous bags, which were stored at room temperature. The CO_2 was measured with gas chromatography (7890A GC System, Agilent Technologies, Santa Clara, CA, USA) within three days. Fluxes were calculated from the linear rate of change in gas concentration, the chamber internal volume, and soil surface area [44].

During the period of December 2010 and April 2011, the R_S, R_H, T_5, and T_{10} were measured using a LI-COR 8100 portable IRGA equipped with a LI-COR 8100-103survey chamber (LI-COR Inc., Lincoln, NE, USA). To avoid the lateral diffusion of CO_2 [33], deep soil collars (determined by snow depth, as did in reference 18) were inserted into the soil surface and stabilized for at least 10 min before measuring the CO_2 efflux. There were four control and four trench-treatment chambers in each plot. The D_S was also measured with a ruler near each chamber of the control plot.

Continuous half-hour means of photosynthetically active radiation (*PAR*), air temperature (T_a), soil temperature at 5 cm (T_5) and 10 cm (T_{10}) depths, and water content at 10 cm depth (SWC_{10}) were measured and recorded in dataloggers (CR1000, Campbell Scientific, Logan, UT, USA), which were equipped with PAR-LITE (Kipp and Zonen, Delft, the Netherlands) at 48 m [39], thermometers (model 107, Campbell Scientific, Logan, UT, USA), and FDRs (EasyAG 50, Sentek, Australia) beneath the flux tower, respectively.

Different methods were used to measure soil CO_2 efflux in the growing and non-growing seasons, i.e., LI-6400 in the growing season, static chamber in the first winter, and LI-8100 in the second winter. We assume that the difference between methods could be ignored. According to Pumpanen et al. [45], the chambers could be sorted into three types: closed static chamber, closed dynamic chamber, and open dynamic chamber. The static chamber could underestimate CO_2 efflux, mainly due to the rising concentration within the chamber headspace [45]. Therefore, we only used this technique in the winter, when CO_2 concentration increases were very small due to the small flux (generally <0.8 µmol m^{-2} s^{-1}). Previous studies verified that the LI-8100 and LI-6400 gave substantially similar results [46,47].

2.2. Data Analysis

Empirical models relating R_S and R_H to soil temperature and water content were developed for each plot, based on discrete measurements of R_S and R_H, soil temperature, and soil water

content (*SWC*), as described in Wang et al. [28,42]. Logarithmic transformation of R_S was needed to achieve linearity and homoscedasticity. A backward elimination procedure was performed to remove insignificant terms ($\alpha > 0.05$). The form of the regression models is

$$\ln(R) = a + b \times T + c \times SWC + d \times T \times SWC \tag{1}$$

where ln is natural logarithm; R represents R_S or R_H; T is the soil temperature; *SWC* is soil water content; and a, b, c, and d are regression coefficients.

The temperature responses of R_S and R_H were regressed by the log-transformed exponential equation

$$\ln(R) = a + b \times T \tag{2}$$

where R is R_S or R_H, and a and b are regression coefficients. Then the temperature coefficient (Q_{10}) was calculated as [48]

$$Q_{10} = e^{10b} \tag{3}$$

Based on a comparison of models with different predictors (Supplementary Materials), we used the T_5 and SWC_{10} to model the growing seasonal fluxes, and the T_5 for the non-growing season. The continuous T_5 and SWC_{10} of the dataloggers were used to estimate the plot-specific T_5 and SWC_{10} with simple linear models. Then the plot-specific T_5 and SWC_{10} were used to drive the respiration models to get half-hour R_S and R_H [28,43]. The seasonal and annual fluxes were the time-integrations of the half-hour R_S and R_H values [24]. The difference in T_5 and SWC_{10} between the treatments was tested by a paired *t*-test at the plot scale (taking the average for each plot and each year). The effect of the difference in SWC_{10} between the treatments was assessed by calculating annual flux in trenched plots (R_H) with the SWC_{10} values in the control and trenched plots [49].Considering the diminishing root decomposition added by the trenching treatment [35], the measurements in the trenched plots were directly considered as R_H. As a result, the R_R was calculated as the difference between R_S and R_H.

In this paper, we report only the data in the last two climatic years for the three plots (numbers 2–4) to quantify the non-growing season contribution and root contribution. One reason was to avoid noncontinuous data, and the other was to minimize the effect of decomposition of newly dead roots after trenching [35].

3. Results

3.1. Seasonal Variations in Soil Respiration and Related Environmental Factors

Both air temperature (T_a) and soil temperature at 5 cm depths (T_5) followed a bell-shaped curve during the study period (Figure 1a). The T_a varied from about -30 °C in January to a maximum of about 23 °C in June. The T_5 generally lagged to the T_a by roughly one month, with a minimum (about -2 °C) in February and a maximum (about 20 °C) in August. Photosynthetically active radiation (*PAR*) peaked slightly earlier than T_a for both growing seasons, but interannually it was lower in mid-to-late summer of 2010. During the winter months, soil volumetric water content in the 10 cm soil layer (SWC_{10}) was low (0.15 m^3 m^{-3}), and increased rapidly following snowmelt in early April (2011) or mid-April (2010; about 0.4 m^3 m^{-3}; Figure 1b). Snow depth (D_S) differed dramatically between the two winters. Snow depth in January was shallower for 2010, but the peak occurred in March (66 cm) for 2010 and in January (41 cm) for 2011 (Figure 1b). The R_S and R_H generally followed the course of T_5 (Figure 1c). The minimum of R_S occurred in February for 2010 and in January for 2011 (0.11 and 0.15 μmol m^{-2} s^{-1}, respectively), and R_H occurred in January for both years (0.09 and 0.06 μmol m^{-2} s^{-1}, respectively). However, R_S maximized in early July while R_H peaked in late July for 2010, whereas R_S and R_H both peaked in mid-August for 2011. The difference in R_S and R_H was generally followed by R_S.
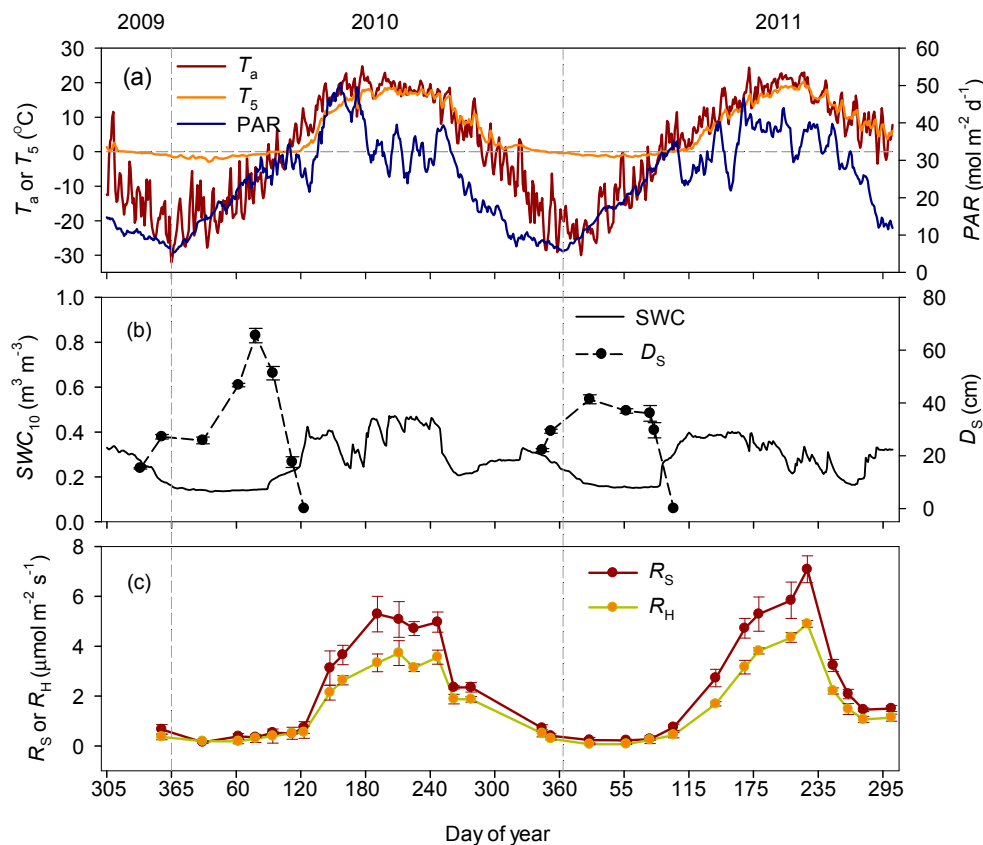
Figure 1. Seasonal dynamics of (**a**) daily air temperature at 16 m height (T_a), daily soil temperature at 5 cm depth (T_5), and daily photosynthetically active radiation (*PAR*); (**b**) daily soil volumetric water content at 0–10 cm depth (SWC_{10}), snow depth (D_S), and (**c**) soil CO_2 efflux (R_S) and CO_2 efflux from trenched plots (R_H) from November 2009 to October 2011. The error bars are standard deviations of the three plots. The vertical dash lines in the figure indicate the end of the year, and the horizontal dash line is zero temperature.

3.2. Responses of Soil Respiration to Soil Temperature and Water Content

Based on the log-transformed exponential model of observed R_S and R_H versus T_5, the R_{S0} and R_{H0} (normalized respiration rate at 0 °C for R_S and R_H) varied between the two non-growing seasons, although R_{S0} was generally higher than R_{H0} (Figure 2). The R_{S0} was higher during the non-growing season between 2009 and 2010 (0.66 μmol m^{-2} s^{-1}) than that during the following non-growing season (0.51 μmol m^{-2} s^{-1}), while R_{H0} was comparable between the two non-growing seasons (0.46 versus 0.42 μmol m^{-2} s^{-1}).The Q_{S10} (Q_{10} for R_S) and Q_{H10} (Q_{10} for R_H) were lower in the non-growing season between 2009 and 2010 than in the following non-growing season. The Q_{S10} was lower than Q_{H10} for both non-growing seasons (18.54 versus 11.13 for the former, and 742.48 versus 152.93 for the latter).

The R_{S0} and R_{H0} for the growing season (0.60–1.00 μmol m^{-2} s^{-1}) were slightly higher than those for the non-growing season (0.42–0.66 μmol m^{-2} s^{-1}), whereas Q_{S10} and Q_{H10} (2.34–3.06) were much lower than those for the non-growing season (11.13–692.29) (Figures 2 and 3). The interannual differences in R_{S0} and R_{H0}, as well as Q_{S10} and Q_{H10} for the growing season, were consistent with those for the non-growing season. For both growing seasons, R_{S0} was higher than R_{H0} and Q_{S10} was larger than Q_{H10}.
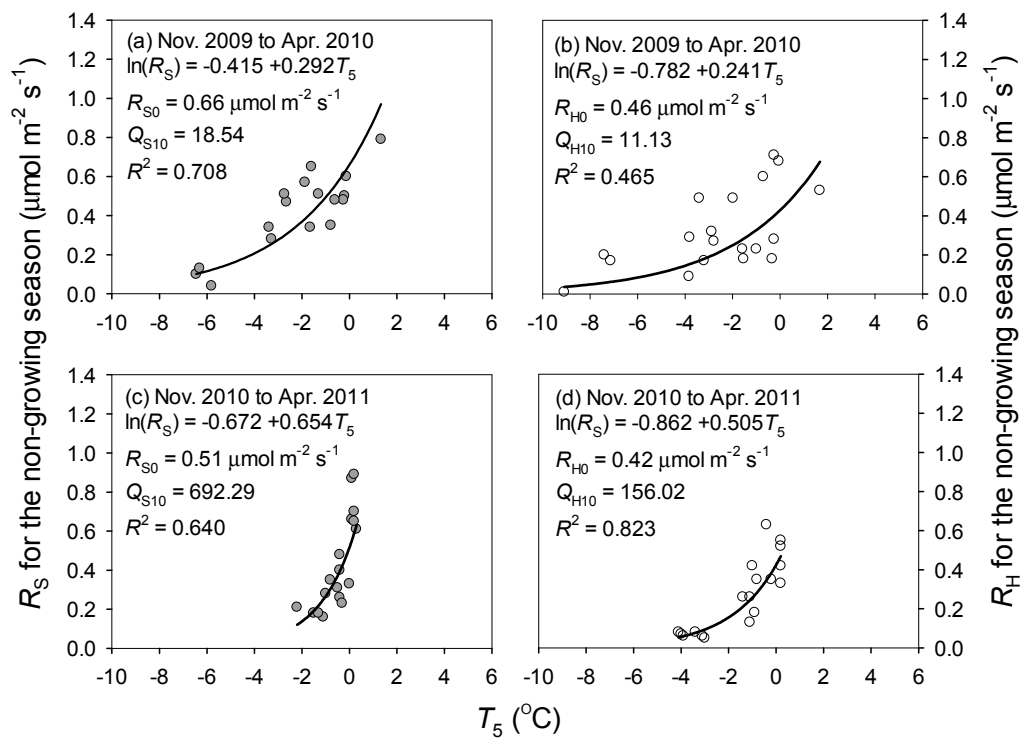
Figure 2. Relationships between soil temperature at 5 cm depth (T_5) and (**a**,**c**) soil CO_2 effluxes (R_S) and (**b**,**d**) CO_2 efflux from trenched plots (R_H) during the non-growing season. The R_{S0} and R_{H0} are normalized respiration rate at 0 °C for R_S and R_H, respectively, and Q_{S10}, Q_{H10} are temperature sensitivities for R_S and R_H, respectively. All *p*-values of the regression models were <0.001.
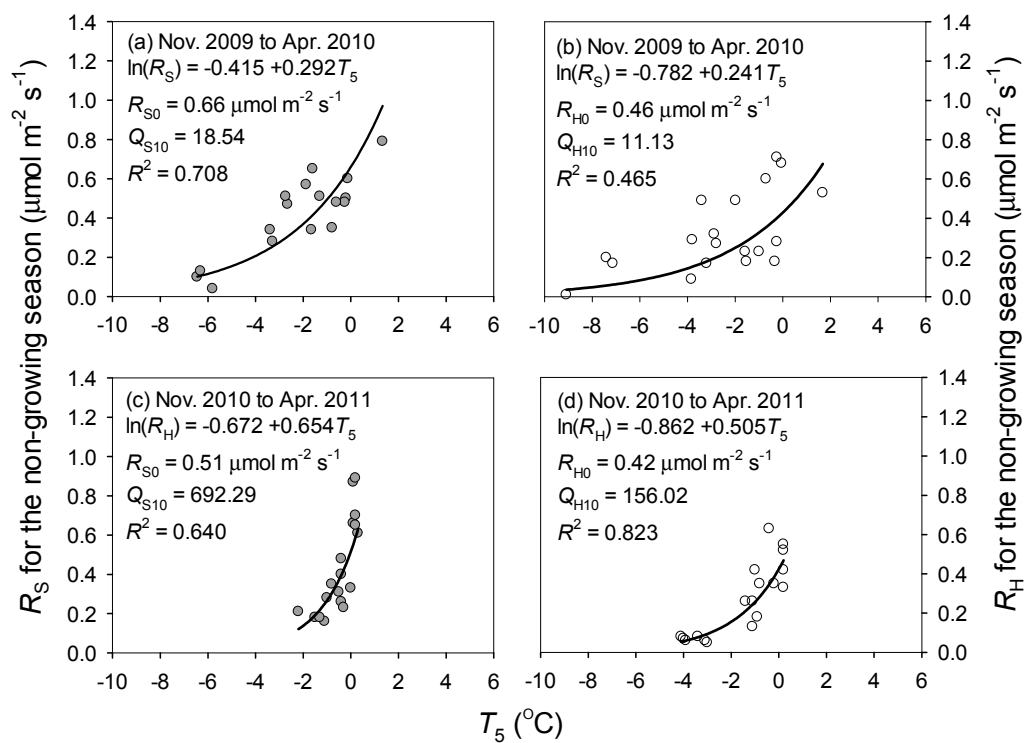

Figure 3. Relationships between soil temperature at 5 cm depth (T_5) and (**a**,**c**) soil CO_2 effluxes (R_S) and (**b**,**d**) CO_2 efflux from trenched plots (R_H) during the growing season. The R_{S0} and R_{H0} are normalized respiration rate at 0 °C for R_S and R_H, respectively, and Q_{S10}, Q_{H10} are temperature sensitivities for R_S and R_H, respectively. All *p*-vales of the regression models were <0.001.

For the growing season, the statistical models of $\ln(R_S)$ and $\ln(R_H)$ against T_5 and SWC_{10} explained 82.5%–91.8% of the variability (Table 2). The R_S and R_H were positively correlated to soil temperature and its interactions with SWC_{10} in all plots for both years, while showed varying correlations to SWC_{10}.

Table 2. Models of soil respiration from control plots (R_S, in µmol m^{-2} s^{-1}) and trenched plots (R_H, in µmol m^{-2} s^{-1}) against soil temperature at 5 cm depth (T_5, in °C), and soil volumetric water content of the top 10 cm (SWC_{10}, in m^3 m^{-3}) for the three plots during the growing season (May to October) for 2010 and 2011.

Year	Variable	Plot	*a*	*b*	*c*	*d*	*N*	*adj.R^2*	*RMSE*
2010	R_S	2	0.44	0.044	−0.837	0.104	72	0.842	0.204
2010	R_S	3	−0.03	0.091			72	0.874	0.163
2010	R_S	4	−0.087	0.092	0.45		72	0.842	0.176
2010	R_H	2	0.281	0.077	−1.181		36	0.827	0.222
2010	R_H	3	−0.178	0.064		0.032	36	0.850	0.151
2010	R_H	4	−0.269	0.085			36	0.833	0.181
2011	R_S	2	−0.715	0.128	2.114		72	0.878	0.219
2011	R_S	3	−0.723	0.112	2.021		72	0.825	0.242
2011	R_S	4	−0.648	0.118	1.976		72	0.855	0.218
2011	R_H	2	−0.502	0.111			36	0.860	0.237
2011	R_H	3	−0.873	0.104	1.654		36	0.918	0.158
2011	R_H	4	−0.545	0.097	0.051		36	0.849	0.227

The regression models are of the form $\ln(R) = a + b \times T_5 + c \times SWC_{10} + d \times T_5 \times SWC_{10}$, where ln is natural logarithm; R is R_S or R_H; and *a*, *b*, *c*, and *d* are significant coefficients ($\alpha = 0.05$). *N*, *adj. R^2*, and *RMSE* are sample size, adjusted determination coefficient, and root mean square error, respectively. All models are highly significant ($p < 0.001$).

3.3. Contribution of Rhizospheric and Heterotrophic Respiration

The contributions of R_H to R_S change with integration period, with the values of 84.8%, 60.7%, and 63.3% for the non-growing season, growing season, and annual period, respectively (Figure 4a). The R_H contribution for the non-growing season was relatively 40% higher than that for growing season.
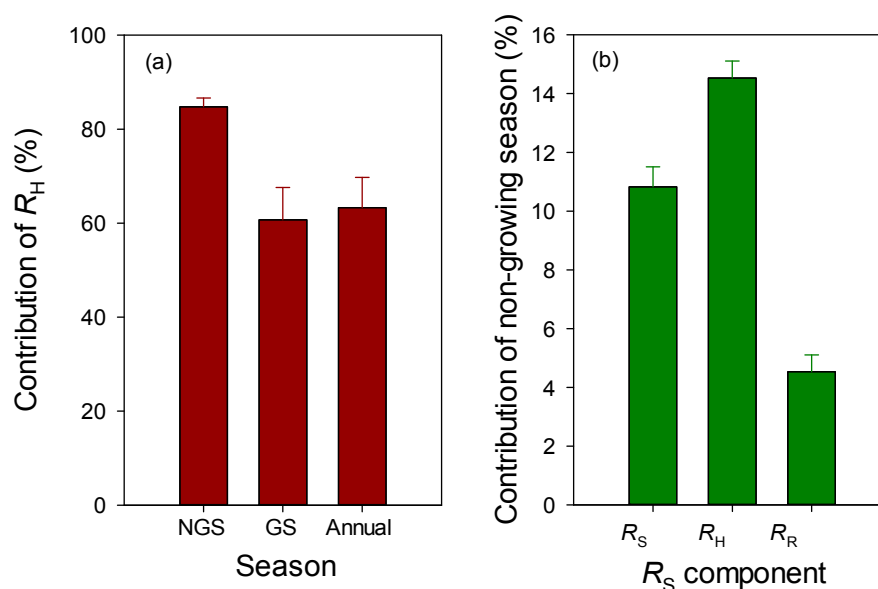

Figure 4. Contributions of the non-growing season to annual (climatic year) respiration for soil (R_S), heterotrophic (R_H), and rhizospheric (R_R) respirations (**a**); the contribution of R_H to R_S for the non-growing season (NGS; from November to April), the growing season (GS; from May to October) and annual fluxes (**b**). The error bars are standard deviations of the three plots.

3.4. Contribution of Non-Growing Season Soil Respiration

The cumulative R_S, R_H, and R_R for the non-growing season range from 84 to 103 g C m^{-2}, from 75 to 84 g C m^{-2}, and from 9 to 19 g C m^{-2}, respectively (Table 3). The mean non-growing season R_S, R_H, and R_R were 94, 79, and 14 g C m^{-2}, respectively. The mean annual R_S, R_H, and R_R were 869, 547, and 321 g C m^{-2} year^{-1}, respectively. The mean R_S, R_H, and R_R for the annual and non-growing season were given in Table S2. Therefore, the non-growing season R_S, R_H, and R_R contributed 10.8%, 14.5%, and 4.5% to the corresponding annual fluxes (Figure 4b). The non-growing season contribution of R_H was twice that of R_R.

Table 3. Cumulative soil surface CO_2 fluxes ($\pm$ standard deviation (SD)) in the control plot (R_S), in the trenched plot (R_H), and rhizospheric respiration (R_R). The means $\pm$ SD of the three plots are given.

Period	Season	Cumulative R_S g C m^{-2}	Cumulative R_H g C m^{-2}	Cumulative R_R g C m^{-2}
November 2009–April 2010	Non-growing season	83.96 $\pm$ 0.99	74.80 $\pm$ 5.19	9.16 $\pm$ 0.82
May 2010–October 2010	Growing season	673.35 $\pm$ 29.26	461.64 $\pm$ 136.25	211.71 $\pm$ 27.75
Nov. 2009–October 2010	Climatic year	757.31 $\pm$ 29.96	536.44 $\pm$ 141.44	220.87 $\pm$ 28.56
November 2010–April 2011	Non-growing season	103.47 $\pm$ 5.33	84.02 $\pm$ 9.91	19.46 $\pm$ 3.42
May 2011–October 2011	Growing season	876.52 $\pm$ 127.96	473.95 $\pm$ 211.10	402.57 $\pm$ 59.49
November 2010–October 2011	Climatic year	979.99 $\pm$ 133.07	557.97 $\pm$ 220.15	422.02 $\pm$ 62.42
	Annual mean	868.65 $\pm$ 78.92	547.20 $\pm$ 179.63	307.14 $\pm$ 31.97

3.5. Effects of Plot Trenching on Soil Respiration and Related Environmental Factors

During the growing season, T_5 was 0.26 °C lower in the control plots than in the trenched plots (12.99 $\pm$ 1.22 °C versus 13.25 $\pm$ 1.36 °C; mean $\pm$ SD; $p = 0.007$),and the trenching effect increased SWC_{10} by 0.05 m^3 m^{-3} (0.30 $\pm$ 0.03 m^3 m^{-3} versus 0.35 $\pm$ 0.04 m^3 m^{-3}; $p = 0.027$). During the non-growing season, trenching significantly decreased T_5 by 0.68 (-0.38 ± 0.35 °C versus -1.06 ± 0.60 °C; $p = 0.011$). However, corrections for differences in T_5 and SWC_{10} did not significantly reduced the CO_2 efflux of the growing season (484 $\pm$ 50 versus 468 $\pm$ 42 g C m^{-2} yr^{-1}; $p = 0.170$).

4. Discussion

4.1. Response of Soil Respiration to Temperature

We found the seasonal variations of R_S and R_H were generally followed by that of T_5, indicating a dominating role of temperature in respiration at the seasonal time scale. However, the different peak timing of R_S and R_H during the former growing season was a response to the lower mid-to-late summer *PAR* (Figure 1). This highlights the importance of a recent supply of assimilates directly to R_R, but not to R_H [11,50,51]. Recently, Zhang et al. [52] verified that changes in photosynthesis drive the seasonal soil respiration–temperature hysteresis relationship, with numerical models and 129 FLUXNET sites. These findings highlight a strong necessity of component partitioning of R_S [8,11,28].

Our estimates in non-growing season R_S (generally <0.8 μmol m^{-2} s^{-1}) was well within the range of previous studies conducted in northern and subalpine forest ecosystems [24,33,53–56]. Higher rates (>0.6 μmol m^{-2} s^{-1}) in a temperate mixed forest in Switzerland may be a result the high soil temperature (roughly above 3 °C) during the dormant season [27]. A lower dormant season R_S in temperate forests (below 0.3 μmol m^{-2} s^{-1}) of North China [18] and in a boreal black spruce forest in Canada [25] may be due to the lower soil temperature, which reached -10 °C at 2 cm depth [25] or 5 cm depth [18] in harsh winter. These results indicated that winter R_S was mainly controlled by soil temperature as at the Maoershan site (Figures 2 and 3).

We found that Q_{S10} and Q_{H10} in the non-growing season were between 11.13 and 692.29, but dropped to between 2.34 and 3.06 in the growing season. Numerous studies have demonstrated exceptionally high Q_{10} for the beneath-snow respiratory flux in cold-winter ecosystems. For instance, the Q_{S10} and Q_{H10} in the dormant season (all above 4) were higher than those in the growing season (often <2) in two forests in the Loess Plateau of China [29]. Although our Q_{s10} of 692.29 might be

unreasonable from a biotic view, a much higher value (1.25×10^6) was reported in a subalpine conifer forest [23]. It has been argued that the high temperature sensitivity could be attributable to the combined effects of exponential growth of snow molds, and the exponential response of their respiration rate to small changes in temperature [57].

Our Q_{S10} was higher than Q_{H10} in both non-growing season. There was a debate on which is higher for Q_{S10} and Q_{H10} in the literature [58,59]. Lower temperature sensitivity for R_S versus R_H was reported in a mixed beech forest in Switzerland during the dormant period [27], in a boreal black spruce plantation in Canada [60], and in an oak chronosequence in China [13]. However, we found that Q_{S10} was more often higher than Q_{H10} in the literature [12,14,25,29,61,62]. The winter higher Q_{S10} compared with Q_{H10} indicated a higher temperature sensitivity of roots than microbes. However, the apparent Q_{10} during the growing season may reflect the effect of plant phenological patterns [48,63,64].

4.2. Non-Growing Season and Annual Soil Respiration

Our mean annual R_S (869 g C m^{-2} yr^{-1}) was similar to that of the previous studies in broadleaved deciduous forests at the same site (781–813 g C m^{-2} yr^{-1}) [38], as well as the mean of global temperate forests (829 $\pm$ 337 g C m^{-2} yr^{-1}) [3]. Our mean accumulated R_S for non-growing seasons (94 g C m^{-2}, Table 3) was also well in the range of the reported values in temperate forests (27–132 g C m^{-2}) [18,54,55,65–67]. Lower R_S values during the non-growing seasons between 2009 and 2010 than those between 2010and 2011 were probably due to the corresponding lower soil temperature (1.6 versus −0.5 for T_5; Figure 1a) [66]. We argue that the interannual variations in soil temperature and the corresponding R_S were mainly due to the difference in D_S before January, rather than the maximum D_S (Figure 1b). Our non-growing season contribution to annual R_S (10.8%) was at the low end of those in literature (6%–23%) [18,24,44,54,66,68–70]. However, the contribution of non-growing season R_H to annual R_H (14.5%) was over triple that of R_R (4.5%). Using the non-growing season R_S contribution to annual R_S (10.8%), to scale growing season measurements, to the annual scale would introduce substantial biases in the annual R_H (−33.70 g C m^{-2} yr^{-1} or −6.2%) and R_R (15.70 g C m^{-2} yr^{-1} or 4.9%).

4.3. Contribution of Rhizospheric and Heterotrophic Respiration

Our annual R_H contribution to R_S (63.3%) was slightly higher than the global means of the temperate deciduous forests: 54% by Subke et al. [35] and ~50% by a recent meta-analysis [14]. Our higher R_H contribution might be due to the relative higher SOC, as indicated by a positive correlation of R_H with the SOC at the same site [28]. However, our estimates of R_H contribution were much higher than those in the broadleaved deciduous forests at the same site (23%–38%) [28]. The discrepancy may be primarily due to different treatment of root decomposition effect.

Heterotrophic contribution varied with the seasons, which might reflect different controlling of R_R and R_H. The R_H dominated R_S (84.8%) in the non-growing season, but its contribution declined in the growing season (60.7%). Similar patterns were widely observed in other northern or subalpine forests [9,12,25,27,29,71]. For example, the contribution of R_H to R_S was lowest in the growing season (54% in an oak forest and 40% in a black locust plantation in the Loess Plateau, China), and it increased up to 88% and 94% during the dormant season [29]. The largest contribution of R_H to R_S was 70% during the dormant period, and as low as 41% during the summer in a mountain mixed temperate forest [27]. In a subalpine ponderosa pine plantation in the United States, the R_H/R_S ratio varied from 44% during the growing season to 84% during the non-growing season [71]. We found that using the R_H contribution during the growing season to estimate the non-growing R_H and R_R would underestimate R_H but overestimate R_R by 22.51 g C m^{-2} yr^{-1}, or 7%. The colder soil in the former winter had a higher R_H contribution versus the latter (89.1% versus 81.3%), although the lower soil temperature suppressed the R_S and its components (Table 3). Reduced winter R_S was widely reported in snow removal experiments [24,54], and between years in natural conditions [66], but the partitioning of R_S is rarely reported. The reduced total respiration but increased R_H contribution indicates a higher

temperature sensitivity of roots versus microbes. This is also supported by the higher Q_{S10} versus Q_{H10} (Figure 3). Therefore, a single value of R_H contribution from growing season measurements should not be applied throughout an annual cycle [9].

4.4. Effects of Plot Trenching on Soil Respiration

The decomposition of dead roots in trenched subplots is one of the most important uncertainties in R_S partitioning. Estimates of this effect in the literature have ranged from 2% to 54% [28,30,35,42,72], with the effect being the most pronounced within the first year after trenching, and declining to minimal levels after two years [26,73] or more [74,75]. The estimate of error introduced by the additional decay of trenched roots for the second year following trenching indicates that R_H might be overestimated by as much as 20% in boreal forests [34] and 14% in temperate forests [64]. The root decomposition accounted for 23%–35% of the annual R_S in a previous study at our site [28], which might be overcorrected due to (1) overestimation of coarse root biomass using allometric equations, which did not account for the declination of root biomass with increasing distance from the stump; and (2) ignoring the carbon input of fine root mortality in natural conditions [76,77]. These uncertainties in dead root decomposition and fine root mortality cautions future studies involving the trenching method [49,73,76,77].

To minimize the effect of root decomposition, we used the measurements in the third and fourth years after trenching, as done in some previous studies (e.g., [61,78]). However, measurements conducted many years after trenching might underestimate the R_H/R_S ratio, due to a lack of below-ground litter input in trenched subplots compared with control plots [35]. Furthermore, eliminating the priming effect of root inputs in trenched plots may decrease decomposition [79], and thus underestimate R_H. Therefore, we did not exclude the root decomposition in the trenched plots. Accurate estimates of R_H by trenching experiment need detailed carbon budgets in trenched plots [77].

Differences in soil moisture and temperature between control and trenched plots may be another potential artifact of the trenching experiment [28,49]. The increase in T_5 by trenching treatment was due to the removal of understory vegetations, which enhances the light reception of the forest floor. However, the trenching effect on T_5 reversed in the non-growing season, which might be attributed to the shallower snowpack or the disturbance introduced when measuring CO_2 efflux. The increase of SWC_{10} (3% or 0.05 m^3 m^{-3}) by trenching might be caused by different soil drainage conditions and water uptake by trees between plots. A previous study reported that the effect of soil moisture was 16% in a pine forest in Sweden [73]. Nevertheless, R_H and its contribution to R_S, based on our plot-specific T_5 and SWC_{10} data and the plot-treatment-specific respiration models, may not be largely influenced by these environmental changes from trenching, because the regression models and the driving variables had already accounted for those changes.

5. Conclusions

Soil rhizospheric and heterotrophic respiration in a temperate deciduous forest was partitioned by a trenching experiment throughout two years. The non-growing seasons' Q_{S10} and Q_{H10} were both much higher than those in the growing season. Mean non-growing season R_S, R_H, and R_R for the two years was 94, 79, and 14 g C m^{-2}, respectively, which contributed 10.8%, 14.5%, and 4.5% to the corresponding annual fluxes (869, 547, and 321 g C m^{-2} yr^{-1}, respectively). The contributions of R_H to R_S for the non-growing season, growing season, and annual period were 81.3%, 60.7%, and 63.3%, respectively. Using the fixed non-growing season contribution of R_S to scale growing season measurements to the annual scale would introduce significant biases on annual R_H (−34 g C m^{-2} yr^{-1} or −6%) and R_R (16 g C m^{-2} yr^{-1} or 5%), and using the R_H contribution measured in the growing season to partitioning R_S in the non-growing season would overestimate R_R by 23 g C m^{-2} yr^{-1} (7% of annual flux). We concluded that it was important to take non-growing season measurements on the partitioning of R_S components in temperate forests.

References

1. Bond-Lamberty, B.; Thomson, A. Temperature-associated increases in the global soil respiration record. *Nature* **2010**, *464*, 579–582. [CrossRef] [PubMed]

2. Hashimoto, S.; Carvalhais, N.; Ito, A.; Migliavacca, M.; Nishina, K.; Reichstein, M. Global spatiotemporal distribution of soil respiration modeled using a global database. *Biogeosciences* **2015**, *12*, 4121–4132. [CrossRef]

3. Hursh, A.; Ballantyne, A.; Cooper, L.; Maneta, M.; Kimball, J.; Watts, J. The sensitivity of soil respiration to soil temperature, moisture, and carbon supply at the global scale. *Glob. Chang. Biol.* **2017**, *23*, 2090–2103. [CrossRef]

4. Beer, C.; Reichstein, M.; Tomelleri, E.; Ciais, P.; Jung, M.; Carvalhais, N.; Rödenbeck, C.; Arain, M.A.; Baldocchi, D.; Bonan, G.B.; et al. Terrestrial gross carbon dioxide uptake: Global distribution and covariation with climate. *Science* **2010**, *329*, 834–838. [CrossRef]

5. Bond-Lamberty, B.; Thomson, A. A global database of soil respiration data. *Biogeosciences* **2010**, *7*, 1915–1926. [CrossRef]

6. Chen, S.; Huang, Y.; Xie, W.; Zou, J.; Lu, Y.; Hu, Z. A new estimate of global soil respiration from 1970 to 2008. *Chin. Sci. Bull.* **2013**, *58*, 4153–4160. [CrossRef]

7. Zhao, Z.; Peng, C.; Yang, Q.; Meng, F.-R.; Song, X.; Chen, S.; Epule, T.E.; Li, P.; Zhu, Q. Model prediction of biome-specific global soil respiration from 1960 to 2012. *Earth's Future* **2017**, *5*, 715–729. [CrossRef]

8. Scott-Denton, L.E.; Rosenstiel, T.N.; Monson, R.K. Differential controls by climate and substrate over the heterotrophic and rhizospheric components of soil respiration. *Glob. Chang. Biol.* **2006**, *12*, 205–216. [CrossRef]

9. Hanson, P.; Edwards, N.; Garten, C.; Andrews, J. Separating root and soil microbial contributions to soil respiration: A review of methods and observations. *Biogeochemistry* **2000**, *48*, 115–146. [CrossRef]

10. Bond-Lamberty, B.; Wang, C.; Gower, S.T. A global relationship between the heterotrophic and autotrophic components of soil respiration? *Glob. Chang. Biol.* **2004**, *10*, 1756–1766. [CrossRef]

11. Högberg, P.; Nordgren, A.; Buchmann, N.; Taylor, A.F.; Ekblad, A.; Högberg, M.N.; Nyberg, G.; Ottosson-Löfvenius, M.; Read, D.J. Large-scale forest girdling shows that current photosynthesis drives soil respiration. *Nature* **2001**, *411*, 789–792. [CrossRef] [PubMed]

12. Savage, K.; Davidson, E.; Tang, J. Diel patterns of autotrophic and heterotrophic respiration among phenological stages. *Glob. Chang. Biol.* **2013**, *19*, 1151–1159. [CrossRef] [PubMed]

13. Luan, J.; Liu, S.; Wang, J.; Zhu, X.; Shi, Z. Rhizospheric and heterotrophic respiration of a warm-temperate oak chronosequence in China. *Soil Biol. Biochem.* **2011**, *43*, 503–512. [CrossRef]

14. Wang, W.; Chen, W.; Wang, S. Forest soil respiration and its heterotrophic and autotrophic components: Global patterns and responses to temperature and precipitation. *Soil Biol. Biochem.* **2010**, *42*, 1236–1244.

15. Bond-Lamberty, B.; Bailey, V.L.; Chen, M.; Gough, C.M.; Vargas, R. Globally rising soil heterotrophic respiration over recent decades. *Nature* **2018**, *560*, 80–83. [CrossRef] [PubMed]

16. Trumbore, S. Carbon respired by terrestrial ecosystems-recent progress and challenges. *Glob. Chang. Biol.* **2006**, *12*, 141–153. [CrossRef]

17. Ryan, M.G.; Law, B.E. Interpreting, measuring, and modeling soil respiration. *Biogeochemistry* **2005**, *73*, 3–27. [CrossRef]

18. Wang, W.; Peng, S.; Wang, T.; Fang, J. Winter soil CO_2 efflux and its contribution to annual soil respiration in different ecosystems of a forest-steppe ecotone, north China. *Soil Biol. Biochem.* **2010**, *42*, 451–458. [CrossRef]

19. Campbell, J.L.; Mitchell, M.J.; Groffman, P.M.; Christenson, L.M.; Hardy, J.P. Winter in northeastern North America: A critical period for ecological processes. *Front. Ecol. Environ.* **2005**, *3*, 314–322. [CrossRef]

20. Sullivan, P.F.; Welker, J.M.; Arens, S.J.T.; Sveinbjörnsson, B. Continuous estimates of CO_2 efflux from arctic and boreal soils during the snow-covered season in Alaska. *J. Geophys. Res.* **2008**, *113*, G04009. [CrossRef]

21. Nobrega, S.; Grogan, P. Deeper snow enhances winter respiration from both plant-associated and bulk soil carbon pools in birch hummock tundra. *Ecosystems* **2007**, *10*, 419–431. [CrossRef]

22. Brooks, P.D.; McKnight, D.; Elder, K. Carbon limitation of soil respiration under winter snowpacks: Potential feedbacks between growing season and winter carbon fluxes. *Glob. Chang. Biol.* **2004**, *11*, 231–238. [CrossRef]

23. Monson, R.K.; Lipson, D.L.; Burns, S.P.; Turnipseed, A.A.; Delany, A.C.; Williams, M.W.; Schmidt, S.K. Winter forest soil respiration controlled by climate and microbial community composition. *Nature* **2006**, *439*, 711–714. [CrossRef]

24. Wang, C.; Han, Y.; Chen, J.; Wang, X.; Zhang, Q.; Bond-Lamberty, B. Seasonality of soil CO_2 efflux in a temperate forest: Biophysical effects of snowpack and spring freeze–thaw cycles. *Agric. For. Meteorol.* **2013**, *177*, 83–92. [CrossRef]

25. Gaumont-Guay, D.; Black, T.A.; Barr, A.G.; Jassal, R.S.; Nesic, Z. Biophysical controls on rhizospheric and heterotrophic components of soil respiration in a boreal black spruce stand. *Tree Physiol.* **2008**, *28*, 161–171. [CrossRef] [PubMed]

26. Lee, M.; Nakane, K.; Nakatsubo, T.; Koizumi, H. Seasonal changes in the contribution of root respiration to total soil respiration in a cool-temperate deciduous forest. *Plant Soil* **2003**, *255*, 311–318. [CrossRef]

27. Ruehr, N.K.; Buchmann, N. Soil respiration fluxes in a temperate mixed forest: Seasonality and temperature sensitivities differ among microbial and root–rhizosphere respiration. *Tree Physiol.* **2010**, *30*, 165–176. [CrossRef]

28. Wang, C.; Yang, J. Rhizospheric and heterotrophic components of soil respiration in six Chinese temperate forests. *Glob. Chang. Biol.* **2007**, *13*, 123–131. [CrossRef]

29. Shi, W.Y.; Zhang, J.G.; Yan, M.J.; Yamanaka, N.; Du, S. Seasonal and diurnal dynamics of soil respiration fluxes in two typical forests on the semiarid Loess Plateau of China: Temperature sensitivities of autotrophs and heterotrophs and analyses of integrated driving factors. *Soil Biol. Biochem.* **2012**, *52*, 99–107. [CrossRef]

30. Brown, R.; Markewitz, D. Soil heterotrophic respiration: Measuring and modeling seasonal variation and silvicultural impacts. *For. Ecol. Manag.* **2018**, *430*, 594–608. [CrossRef]

31. Carbone, M.S.; Richardson, A.D.; Chen, M.; Davidson, E.A.; Hughes, H.; Savage, K.E.; Hollinger, D.Y. Constrained partitioning of autotrophic and heterotrophic respiration reduces model uncertainties of forest ecosystem carbon fluxes but not stocks. *J. Geophys. Res. Biogeosci.* **2016**, *121*, 2476–2492. [CrossRef]

32. Tucker, C.; Young, J.; Williams, D.; Ogle, K. Process-based isotope partitioning of winter soil respiration in a subalpine ecosystem reveals importance of rhizospheric respiration. *Biogeochemistry* **2014**, *121*, 389–408. [CrossRef]

33. Schindlbacher, A.; Zechmeister-Boltenstern, S.; Glatzel, G.; Jandl, R. Winter soil respiration from an Austrian mountain forest. *Agric. For. Meteorol.* **2007**, *146*, 205–215. [CrossRef]

34. Bond-Lamberty, B.; Wang, C.; Gower, S.T. Contribution of root respiration to soil surface CO_2 flux in a boreal black spruce chronosequence. *Tree Physiol.* **2004**, *24*, 1387–1395. [CrossRef] [PubMed]

35. Subke, J.A.; Inglima, I.; Francesca Cotrufo, M. Trends and methodological impacts in soil CO_2 efflux partitioning: A metaanalytical review. *Glob. Chang. Biol.* **2006**, *12*, 921–943. [CrossRef]

36. Kuzyakov, Y. Sources of CO_2 efflux from soil and review of partitioning methods. *Soil Biol. Biochem.* **2006**, *38*, 425–448. [CrossRef]

37. Liu, F.; Wang, C.; Wang, X.; Zhang, J.; Zhang, Z.; Wang, J. Spatial patterns of biomass in the temperate broadleaved deciduous forest within the fetch of the Maoershan flux tower. *Acta Ecol. Sin.* **2016**, *36*, 6506–6519.

38. Liu, Z.; Wang, C.; Chen, J.M.; Wang, X.; Jin, G. Empirical models for tracing seasonal changes in leaf area index in deciduous broadleaf forests by digital hemispherical photography. *For. Ecol. Manag.* **2015**, *351*, 67–77. [CrossRef]

39. Liu, F.; Wang, C.; Wang, X. Monitoring temporal dynamics in leaf area index of the temperate broadleaved deciduous forest in Maoershan region with tower-based radiation measurements. *Chin. J. Appl. Ecol.* **2016**, *27*, 2409–2419.

40. Kong, Q.; Wang, C.; Wang, X. Effects of detritus removal on soil carbon, nitrogen and phosphorus stoichiometry and related factors in a temperate deciduous forest in the Maoershan Mountain, China. *Chin. J. Appl. Ecol.* **2018**, *29*, 2173–2182.

41. Jassal, R.S.; Black, T.A. Estimating heterotrophic and autotrophic soil respiration using small-area trenched plot technique: Theory and practice. *Agric. For. Meteorol.* **2006**, *140*, 193–202. [CrossRef]

42. Wang, C.; Yang, J.; Zhang, Q. Soil respiration in six temperate forests in China. *Glob. Chang. Biol.* **2006**, *12*, 2103–2114. [CrossRef]

43. Davidson, E.; Savage, K.; Verchot, L.; Navarro, R. Minimizing artifacts and biases in chamber-based measurements of soil respiration. *Agric. For. Meteorol.* **2002**, *113*, 21–37. [CrossRef]

44. Groffman, P.M.; Hardy, J.P.; Driscoll, C.T.; Fahey, T.J. Snow depth, soil freezing, and fluxes of carbon dioxide, nitrous oxide and methane in a northern hardwood forest. *Glob. Chang. Biol.* **2006**, *12*, 1748–1760. [CrossRef]

45. Xu, M.; Qi, Y. Soil-surface CO_2 efflux and its spatial and temporal variations in a young ponderosa pine plantation in northern California. *Glob. Chang. Biol.* **2001**, *7*, 667–677. [CrossRef]

46. Pumpanen, J.; Kolari, P.; Ilvesniemi, H.; Minkkinen, K.; Vesala, T.; Niinistö, S.; Lohila, A.; Larmola, T.; Morero, M.; Pihlatie, M.; et al. Comparison of different chamber techniques for measuring soil CO_2 efflux. *Agric. For. Meteorol.* **2004**, *123*, 159–176. [CrossRef]

47. Madsen, R.A.; Demetriades-Shah, T.H.; Garcia, R.L.; McDermitt, D.K. *Soil CO_2 Flux Measurements: Comparisons between the LI-COR LI-6400 and LI-8100*; Technical Note; LI-COR Biosciences: Lincoln, NE, USA, 2004.

48. Reinmann, A.B.; Templer, P.H. Increased soil respiration in response to experimentally reduced snow cover and increased soil freezing in a temperate deciduous forest. *Biogeochemistry* **2018**, *140*, 359–371. [CrossRef]

49. Ngao, J.; Longdoz, B.; Granier, A.; Epron, D. Estimation of autotrophic and heterotrophic components of soil respiration by trenching is sensitive to corrections for root decomposition and changes in soil water content. *Plant Soil* **2007**, *301*, 99–110. [CrossRef]

50. Moyano, F.E.; Kutsch, W.L.; Rebmann, C. Soil respiration fluxes in relation to photosynthetic activity in broad-leaf and needle-leaf forest stands. *Agric. For. Meteorol.* **2008**, *148*, 135–143. [CrossRef]

51. Sampson, D.A.; Janssens, I.A.; Curiel yuste, J.; Ceulemans, R. Basal rates of soil respiration are correlated with photosynthesis in a mixed temperate forest. *Glob. Chang. Biol.* **2007**, *13*, 2008–2017. [CrossRef]

52. Zhang, Q.; Phillips, R.P.; Manzoni, S.; Scott, R.L.; Oishi, A.C.; Finzi, A.; Daly, E.; Vargas, R.; Novick, K.A. Changes in photosynthesis and soil moisture drive the seasonal soil respiration-temperature hysteresis relationship. *Agric. For. Meteorol.* **2018**, *259*, 184–195. [CrossRef]

53. Suzuki, S.; Ishizuka, S.; Kitamura, K.; Yamanoi, K.; Nakai, Y. Continuous estimation of winter carbon dioxide efflux from the snow surface in a deciduous broadleaf forest. *J. Geophys. Res.* **2006**, *111*, D17101. [CrossRef]

54. Gao, D.; Hagedorn, F.; Zhang, L.; Liu, J.; Qu, G.; Sun, J.; Peng, B.; Fan, Z.; Zheng, J.; Jiang, P.; et al. Small and transient response of winter soil respiration and microbial communities to altered snow depth in a mid-temperate forest. *Appl. Soil Ecol.* **2018**, *130*, 40–49. [CrossRef]

55. Hubbard, R.M.; Ryan, M.G.; Elder, K.; Rhoades, C.C. Seasonal patterns in soil surface CO_2 flux under snow cover in 50 and 300 year old subalpine forests. *Biogeochemistry* **2005**, *73*, 93–107. [CrossRef]

56. Du, E.; Zhou, Z.; Li, P.; Jiang, L.; Hu, X.; Fang, J. Winter soil respiration during soil-freezing process in a boreal forest in Northeast China. *J. Plant Ecol.* **2013**, *6*, 349–357. [CrossRef]

57. Schmidt, S.; Wilson, K.; Monson, R.; Lipson, D. Exponential growth of "snow molds" at sub-zero temperatures: An explanation for high beneath-snow respiration rates and Q_{10} values. *Biogeochemistry* **2009**, *95*, 13–21. [CrossRef]

58. Högberg, P. Is tree root respiration more sensitive than heterotrophic respiration to changes in soil temperature? *New Phytol.* **2010**, *188*, 9–10. [CrossRef]

59. Luo, Y.; Zhou, X. Deconvolution analysis to quantify autotrophic and heterotrophic respiration and their temperature sensitivities. *New Phytol.* **2010**, *188*, 10–11. [CrossRef]

60. Bond-Lamberty, B.; Bronson, D.; Bladyka, E.; Gower, S.T. A comparison of trenched plot techniques for partitioning soil respiration. *Soil Biol. Biochem.* **2011**, *43*, 2108–2114. [CrossRef]

61. Boone, R.D.; Nadelhoffer, K.J.; Canary, J.D.; Kaye, J.P. Roots exert a strong influence on the temperature sensitivity of soil respiration. *Nature* **1998**, *396*, 570–572. [CrossRef]

62. Jiang, L.; Shi, F.; Li, B.; Luo, Y.; Chen, J.; Chen, J. Separating rhizosphere respiration from total soil respiration in two larch plantations in northeastern China. *Tree Physiol.* **2005**, *25*, 1187–1195. [CrossRef] [PubMed]

63. Curiel Yuste, J.; Janssens, I.A.; Carrara, A.; Ceulemans, R. Annual Q_{10} of soil respiration reflects plant phenological patterns as well as temperature sensitivity. *Glob. Chang. Biol.* **2004**, *10*, 161–169. [CrossRef]

64. Davidson, E.A.; Janssens, I.A. Temperature sensitivity of soil carbon decomposition and feedbacks to climate change. *Nature* **2006**, *440*, 165–173. [CrossRef] [PubMed]

65. McDowell, N.G.; Marshall, J.D.; Hooker, T.D.; Musselman, R. Estimating CO_2 flux from snowpacks at three sites in the Rocky Mountains. *Tree Physiol.* **2000**, *20*, 745–753. [CrossRef] [PubMed]

66. Ruehr, N.K.; Knohl, A.; Buchmann, N. Environmental variables controlling soil respiration on diurnal, seasonal and annual time-scales in a mixed mountain forest in Switzerland. *Biogeochemistry* **2010**, *98*, 153–170. [CrossRef]

67. Mo, W.; Lee, M.S.; Uchida, M.; Inatomi, M.; Saigusa, N.; Mariko, S.; Koizumi, H. Seasonal and annual variations in soil respiration in a cool-temperate deciduous broad-leaved forest in Japan. *Agric. For. Meteorol.* **2005**, *134*, 81–94. [CrossRef]

68. Kim, Y.; Ueyama, M.; Nakagawa, F.; Tsunogai, U.; Tanaka, N.; Harazono, Y. Assessment of winter fluxes of CO_2 and CH_4 in boreal forest soils of central Alaska estimated by the profile method and the chamber method: A diagnosis of methane emission and implications for the regional carbon budget. *Tellus B* **2007**, *59*, 223–233. [CrossRef]

69. Wang, C.; Bond-Lamberty, B.; Gower, S.T. Soil surface CO_2 flux in a boreal black spruce fire chronosequence. *J. Geophys. Res.* **2002**, *108*, 8224. [CrossRef]

70. Vogel, J.G.; Valentine, D.W.; Ruess, R.W. Soil and root respiration in mature Alaskan black spruce forests that vary in soil organic matter decomposition rates. *Can. J. For. Res.* **2005**, *35*, 161–174. [CrossRef]

71. Tang, J.; Misson, L.; Gershenson, A.; Cheng, W.; Goldstein, A.H. Continuous measurements of soil respiration with and without roots in a ponderosa pine plantation in the Sierra Nevada Mountains. *Agric. For. Meteorol.* **2005**, *132*, 212–227. [CrossRef]

72. Saiz, G.; Byrne, K.A.; Butterbach-Bahl, K.; Kiese, R.; Blujdea, V.; Farrell, E.P. Stand age-related effects on soil respiration in a first rotation Sitka spruce chronosequence in central Ireland. *Glob. Chang. Biol.* **2006**, *12*, 1007–1020. [CrossRef]

73. Comstedt, D.; Boström, B.; Ekblad, A. Autotrophic and heterotrophic soil respiration in a Norway spruce forest: Estimating the root decomposition and soil moisture effects in a trenching experiment. *Biogeochemistry* **2011**, *104*, 121–132. [CrossRef]

74. Díaz-Pinés, E.; Schindlbacher, A.; Pfeffer, M.; Jandl, R.; Zechmeister-Boltenstern, S.; Rubio, A. Root trenching: A useful tool to estimate autotrophic soil respiration? A case study in an Austrian mountain forest. *Eur. J. For. Res.* **2010**, *129*, 101–109. [CrossRef]

75. Epron, D.; Farque, L.; Lucot, E.; Badot, P.M. Soil CO_2 efflux in a beech forest: The contribution of root respiration. *Ann. For. Sci.* **1999**, *56*, 289–295. [CrossRef]

76. Varik, M.; Kukumägi, M.; Aosaar, J.; Becker, H.; Ostonen, I.; Lõhmus, K.; Uri, V. Carbon budgets in fertile silver birch (*Betula pendula* Roth) chronosequence stands. *Ecol. Eng.* **2015**, *77*, 284–296. [CrossRef]

77. Kukumägi, M.; Ostonen, I.; Uri, V.; Helmisaari, H.S.; Kanal, A.; Kull, O.; Lõhmus, K. Variation of soil respiration and its components in hemiboreal Norway spruce stands of different ages. *Plant Soil* **2017**, *414*, 265–280. [CrossRef]

78. Sulzman, E.W.; Brant, J.B.; Bowden, R.D.; Lajtha, K. Contribution of aboveground litter, belowground litter, and rhizosphere respiration to total soil CO_2 efflux in an old growth coniferous forest. *Biogeochemistry* **2005**, *73*, 231–256. [CrossRef]

79. Kuzyakov, Y. Priming effects: Interactions between living and dead organic matter. *Soil Biol. Biochem.* **2010**, *42*, 1363–1371. [CrossRef]